Proceedings of ERAD 2006

Filtering weather radar AP echoes with MSG observations and NWP data

A. Magaldi [1], J. Bech [1,2], G. Delgado[1], J. Lorente[1]

[1]Departament d'Astronomia i Meteorologia-Universitat de Barcelona, Barcelona (Spain).

[2] Meteocat, Berlin 38, 4th. E-08029, Barcelona (Spain).

1 Introduction

The propagation of the electromagnetic waves in the atmosphere depends mainly on the atmospheric refractive index (n).

Since small changes in n can cause important effects in the radar propagation the concept of refractivity (N) is commonly used. According to Bean and Dutton (1968) N is defined as:

$$N = 77.6\frac{p}{T} - 5.6e + 3.75\times10^{5}\frac{e}{T^{2}} \qquad (1)$$

where p is the atmospheric pressure (hPa), T the temperature (K) and e is the water vapor partial pressure (hPa).

Therefore, if the atmospheric vertical profile of the previous variables is known, then the propagation path of the electromagnetic waves emitted by the radar can be determined.

The equation that describes the ratio between the radar ray curvature (r) in the atmosphere and Earth radius (R_e) is known as effective Earth radius factor k_e:

$$k_e = \frac{r}{R_e} \approx \frac{1}{1+\left(dN/dh\right)/157} \qquad (2)$$

where (dn/dh) is the vertical refractive index gradient.

Climatological atmospheric observations indicate that statistical normal propagation is associated to vertical refractive index gradients of the first kilometer of the atmosphere (VRG) between -39 and - 40 km^{-1}.

When this condition is verified the beam path of the electromagnetic waves are curved towards the terrestrial surface, with a smaller curvature than the average Earth's surface curvature. Therefore, the trajectory of the waves emitted by the radar gains altitude as it moves away from the radar. This VRG value gives an effective k_e of 4/3 (Fig. 1b).

When the refractivity diminishes with height, the trajectories of the electromagnetic waves are curved away from the ground more than usual. This behavior characterized by k_e < 4/3 is known as sub-refraction (Fig.1a).

When the VRG is ≤ 80 km^{-1} then super-refraction appears. Under this condition the electromagnetic propagation path is turned towards the Earth surface. A super-refraction implies a k_e > 4/3. This situation is known as anomalous propagation (AP). Super-refractive conditions can generate the intersection of the radar beam with the orography causing a spurious radar echo (Fig. 1c).

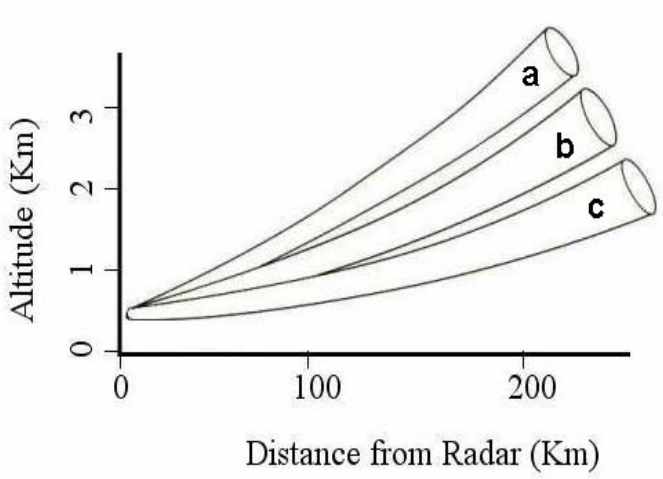

Fig. 1. Schematic height of the beam vs distances in function of VRG (a) sub–refraction, (b) normal and (c) super-refraction.

Correspondence to: A. Magaldi.

amagaldi@am.ub.es

2 Methodology

In order to improve weather radar observations and eliminating spurious echoes originated by AP it was chosen a multisource strategy, which uses the observations of the Meteosat 8 satellite (MSG) and Numerical Weather Prediction (NWP) MASS model data.

The basic principle to "clean" the radar observations is: a radar echo must come from a region where a precipitating cloud is present; otherwise this echo is suspicious of being originated by effects of AP. Two precipitating cloud masks were elaborated adapting the algorithms of Michelson and Sunhede (2004) and SAF (2004), hereafter MS and SAF respectively. These masks were superposed on the radar data to identify which echoes were not coming from a precipitating cloud. These echoes were removed of the radar image because they don't fulfill the basic principle to come from a precipitating cloud region. (Fig. 2 and 3).

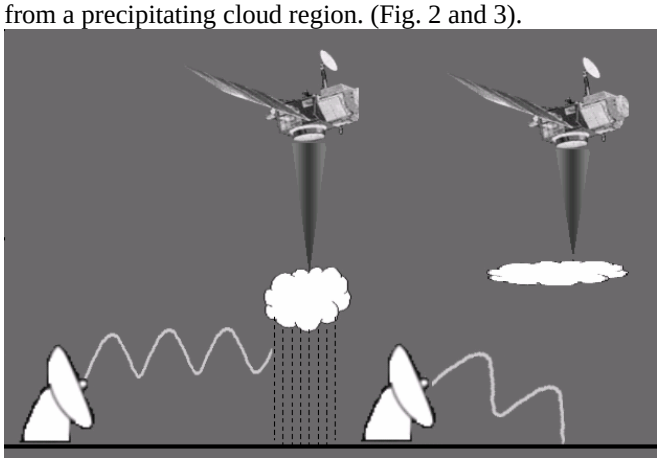

Fig. 2. Scheme of the method used in this work.

2.1 SAF Algorithm

The linear combination of the MSG spectral channels and the surface temperature generated by the NWP model MASS, that have a greater correlation with the precipitation, are used to construct an Index of Percentage of Precipitating Clouds (PPC). For each value of the PPC, the precipitation probability is determined for three intensity classes: 1) No precipitation, 2) Light to moderate precipitation, 3) Heavy precipitation. The likelihood in all three classes has to sum up to 100%. The total likelihood of precipitation is the sum of the likelihood in class 2 and class 3.

In this work we assumed that there is a precipitating cloud when PPC has a probability greater than 85%. This algorithm is inspired in several works developed specifically for the AVHRR (Stowe *et.al*, 1991). The equation behind the PPC is the following one:

$$PPC = a_0 + a_1 T_{2m} + a_2 T_{10.8} + a_3 \ln(R_{0.6} / R_{3.9}) + a_4 (T_{10.8} - T_{12.0}) + a_5 \left| (a_6 - R_{0.6}) / R_{1.6} \right| + a_7 R_{0.6} \quad (3)$$

where T_{2m} is the surface temperature generated by the NWP MASS Model and R and the other Ts respectively denote radiances and brightness temperature (the sub index that appears after the R and T is the central wavelength of the MSG channel expressed in micrometers), and the a_n coefficients are given in Table 1.

2.2 MS Algorithm

This model is based on assuming the next fact: the precipitating clouds are colder and reflect better than the terrestrial surface the light of the sun. Therefore, the difference between surface temperature and brightness temperature are basic in order to identify rain or no rain areas (Ebert and Weymouth, 1999). The conditions of which a cloud can precipitate are given by the fact that one of the following conditions can happen:

$$\left.\begin{array}{ll} T_{2m} - T_{10.8} & \geq 20^{o}C \\ T_{2m} & < -5^{o}C \\ T_{10.8} & < 0^{o}C \end{array}\right\} \Rightarrow \textit{precipitat ing cloud} \quad (4)$$

where the variables use the same notation than in equation 3.

Table 1. Numerical value of the coefficients a_n in the equation 3

	Day	Night
a_0	50.00	22.00
a_1	0.322	0.863
a_2	-0.322	-0.863
a_3	3.00	0.00
a_4	-2.42	0.86
a_5	7.50	-6.04
a_6	4.50	0.00
a_7	0.248	0.00

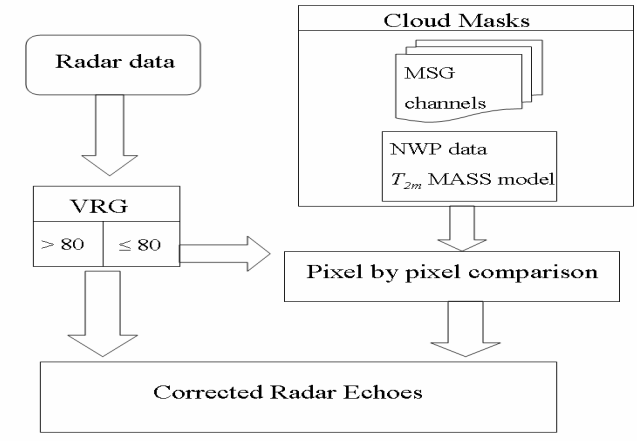

Fig. 3. Data-flow diagram of the methodology used.

3 Results

The methods developed in the present work were evaluated during the period December 2004 - June 2005, using the Vallirana radar of METEOCAT (Bech et al., 2004). Two episodes were selected and verified with gauge data (Fig. 4).

One took place in winter (December 1st and 2nd of 2004) and the other in summer (June 25 th and 26 th). After applying the cloud masks, the corrected images of the radar show a smaller area with presence of echoes. The two techniques show very similar results because the only discrepancy is in the extension of the area with presence of echoes (Fig. 5).

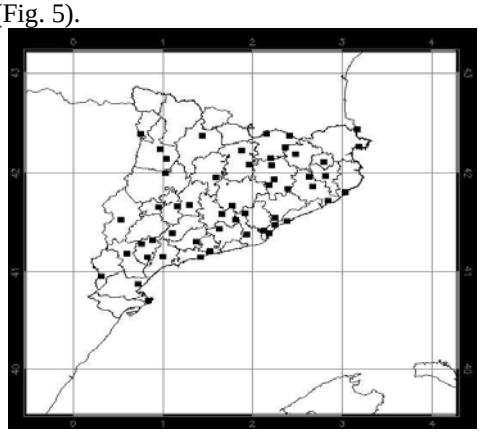

Fig. 4. XMET rain gauge net geographic location

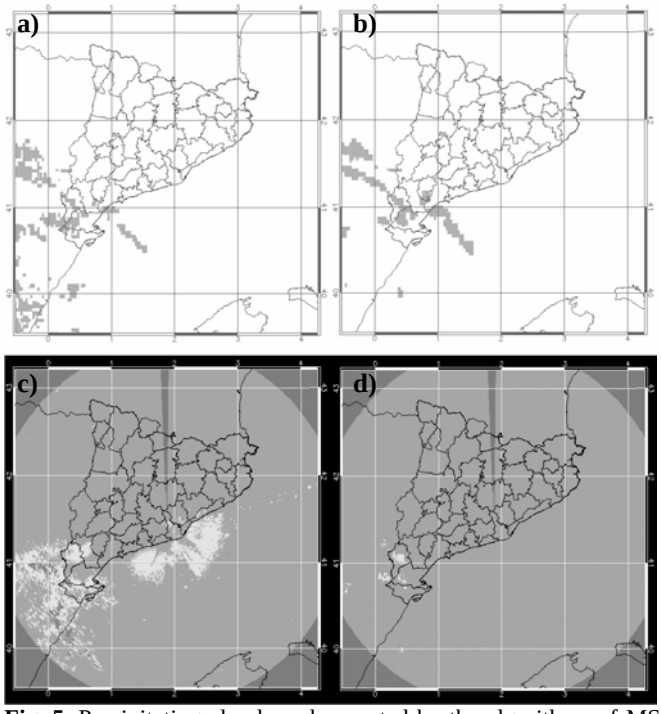

Fig. 5. Precipitating cloud masks created by the algorithms of MS (5a) and SAF (5b). Image of the radar without correction (5c) and the radar corrected by the SAF algorithm (5d) for the 14:00Z of the January 1st. 2004.

Table 3. Percent Correct (PC), False Alarm Rate (FAR), and Hanssen-Kuipers skill (HKS) scores for three echo classes: uncorrected (UC) and corrected by MS and SAF algorithms.

Echo class	FAR			PC			HKS		
	UC	MS	SAF	UC	MS	SAF	UC	MS	SAF
Weak	0.56	0.20	0.10	81.22	93.25	94.52	0.22	0.20	0.24
Strong	0.32	0.26	0.23	70.53	77.09	76.96	0.30	0.24	0.29
All	0.24	0.24	0.20	79.78	85.91	87.13	0.23	0.21	0.26

Table 4. Size of the sample for each echo class.

Echo class	Size of the sample	
	Winter	Spring
Weak	1309	1444
strong	355	412
All	1664	1856

The corrected field of the radar was compared with precipitation data observed from the XMET rain gauge network of METEOCAT. The values of the FAR index are smaller after applying the mask, which implies a decrease in the cases in which the radar detected an echo on a station that did not detect rain. These cases are especially important because it is possible to state that this improvement comes from the elimination of spurious echoes. The values of the PC index improved substantially, particularly for weak echoes. This is reflected in an increase of the cases in which the radar and the rain gauges agreed in their observation. The results of the HKS index suggest an improvement in the probability of correct detection when the SAF method is applied. Further events are necessary to extend the analysis and obtain more conclusive results.

Acknowledgements: We are indebted to Meteosim (www.meteosim.com) for providing the NWP MASS model data and to the Meteorological Service of Catalonia for the radar and rain gauge-data.

References

Bech, J., Vilaclara, E., Pineda, N., Rigo, T., López, J.,O'Hora, F., Lorente, J., Sempere, D., Fàbregas, F. X., 2004: The weather radar network of the Catalan Meteorological Service: description and applications. *European Conference on Radar in Meteorology and Hydrology (ERAD) - COST 717 Final Seminar*, ERAD Publication Series Vol 2. Copernicus GmbH (c) 2004 ISBN 3-936586-29-2, pp. 416-420.

Bean, B. R., and E. J. Dutton, 1968: *Radio Meteorology*. 438 pp, Dover Publications.

Ebert, E. E., and G. T. Weymouth, 1999: Incorporating satellite observations of 'No Rain' in an Australian daily rainfall analysis, *J. Appl. Meteor*., **38**, 44 – 56

Häggmark, K-I., K.I. Ivarsson, S. Gollvik, and P. O. Olofsson, 2000: Mesan an operational mesoscale analysis system, *Tellus.*,**52**,2 20

Michelson, D. B., and D. Sunhede, 2004: Spurious weather radar echo identification and removal using multisource temperature information, *Meteorol. Appl*. **11**, 1-14

SAF, 2004: Software User Manual for PGE04 of the NWCSAF/MSG: Scientific Part, *Eumetsat techmemo*. 30 pp, Eumetsat

Stowe, L. L.. E. P. McClain, R. Carey, P. Pellegrino, G. Gutman. P. Davis, C. Long, and S. Hart, 1991: Global distribution of cloud cover derived from NOAAiAVHRR operational satellite data, *Adv. Space Res.*, **11,** 351-354